

Supporting Information

MoP/Mo₂C@C: a new combination of electrocatalysts for highly efficient hydrogen evolution over all pH range

Lu-Nan Zhang,^{a†} Si-Heng Li,^{a†} Hua-Qiao Tan,^{a} Shifa Ullah Khan,^a Yuan-Yuan Ma,^a Hong-Ying Zang,^{a*} Yong-Hui Wang,^a Yang-Guang Li^{a*}*

Key Laboratory of Polyoxometalate Science of Ministry of Education, Faculty of Chemistry, Northeast Normal University, Changchun, 130024 (P.R. China)

*E-mail: liyg658@nenu.edu.cn; tanhq870@nenu.edu.cn; zanghy100@nenu.edu.cn.

Table of contents

Section	Page
Additional characterization techniques	S3
Characterizations of precursor (Figure S1)	S4
Additional characterizations of MoP/Mo ₂ C@C and control samples (Figure S2-Figure S4, Table S1)	S4
Comparison of HER performance in acidic media for MoP/Mo ₂ C@C with other HER elecrocatalysts (Table S2)	S6
Electrochemical experiments and characterizations of control samples (Figure S5-Figure S11)	S7
Additional electrochemical experiments of MoP/Mo ₂ C@C (Table S3)	S10
Comparison of HER performance in alkaline media for MoP/Mo ₂ C@C with other HER elecrocatalysts (Table S4)	S11
Electrochemical experiments of MoP/Mo ₂ C@C in all pH values (Figure S12-Figure S14, Table S5)	S12
Additional experimental data for comparison	S16

Physical characterization

The electron transmission microscopy (TEM) was performed on a JEOL-2100F transmission electron microscope. The powder X-ray diffraction (PXRD) measurements were carried out on a Rigaku D/max-IIb X-ray diffractometer with Cu-K α radiation ($\lambda=1.5418\text{\AA}$). Raman spectrum was recorded on a Raman spectrometer (JY, Labram HR 800). The X-ray photoelectron spectroscopy (XPS) measurements were performed on an ESCALAB 250 spectrometer (Thermo Electron Corp.) with Al K α radiation ($h\nu = 1486.6$ eV) as the excitation source. The interrelated energy dispersive X-ray detector (EDX) spectra were achieved by using a SU8000 ESEM FEG microscope. The nitrogen sorption measurement was obtained on an ASAP 2020 (Micromeritics, USA).

Electrochemical measurements

All the cyclic voltammetry (CV) and linear sweep voltammetry (LSV) measurements were performed with a typical three-electrode system using a CHI660E electrochemical workstation (CH Instruments, China) at 25 °C. A modified glassy carbon electrode (GCE, d = 3 mm) was served as the working electrode. A carbon rod was used as the counter electrode, and a saturated calomel electrode (SCE) as the reference electrode. For comparison, the bare glassy carbon electrode (GCE) and commercial Pt/C catalyst (20 wt% Pt/XC-72R) are also evaluated as reference samples. In all measurements, the potential measured against an SCE electrode were calibrated to the potentials referenced to the reversible hydrogen electrode (RHE), according to $E_{\text{RHE}} = E_{\text{SCE}} + E^{\circ}_{\text{SCE}} + 0.059\text{pH}$. All the electrolytes were N₂ saturated before the measurements. The linear sweep voltammetry (LSV) measurements were carried out with a scan rate of 5 mV s⁻¹. Tafel slopes were determined by fitting the linear regions of Tafel plots according to the Tafel equation ($\eta = b \log j + a$). Electrochemical stability was measured using cyclic voltammetric sweeps at 100 mV s⁻¹ between + 0.2 V and - 0.2 V (vs. RHE). To evaluate electrochemically active surface area (ECSA), the scan rate of cyclic voltammograms was set to 25, 50, 75, 100, 125, 150, 175, and 200 mV s⁻¹. The range of voltage was from -0.1 to 0.1 V (vs. SCE, in 0.5 M H₂SO₄), -0.5 to -0.3 V (vs. SCE, in 1 M PBS), and -1.1 to -0.9 V (vs. SCE, in 1 M KOH), respectively. The long-term (14 h) stability was also tested at controlled overpotential. Electrochemical impedance spectroscopy (EIS) was performed on a PARSTAT 2273 electrochemical configuration (Princeton Applied Research Instrumentation, USA) with frequency from 0.01 to 100000 Hz and an amplitude of 10 mV. The EIS spectra were fitted by the Z-SimpWin software. All the electrochemistry measurements are represented with IR compensation.

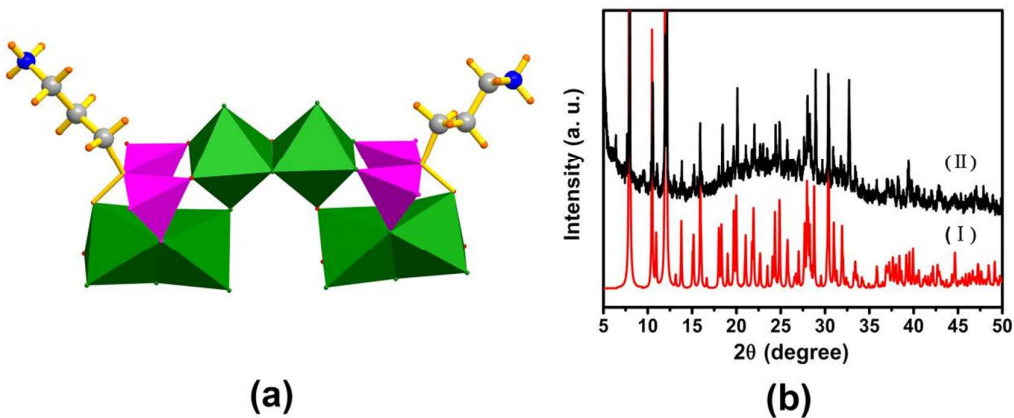


Figure S1 (a) Polyhedral and ball-and-stick representation of polyoxoanion in P_4Mo_6 precursor $(\text{NH}_4)_6 \{ \text{Mo}_2\text{O}_4 [(\text{Mo}_2\text{O}_6)\text{NH}_3\text{CH}_2\text{CH}_2\text{CH}_2\text{C}(\text{O})(\text{PO}_3)_2]_2 \} \cdot 10\text{H}_2\text{O}$; (b) Powder XRD patterns of P_4Mo_6 : (I) simulated; (II) as-synthesized P_4Mo_6 . The peak positions of simulated and experimental patterns of P_4Mo_6 are in agreement with each other, indicating the phase purity and good crystallinity.

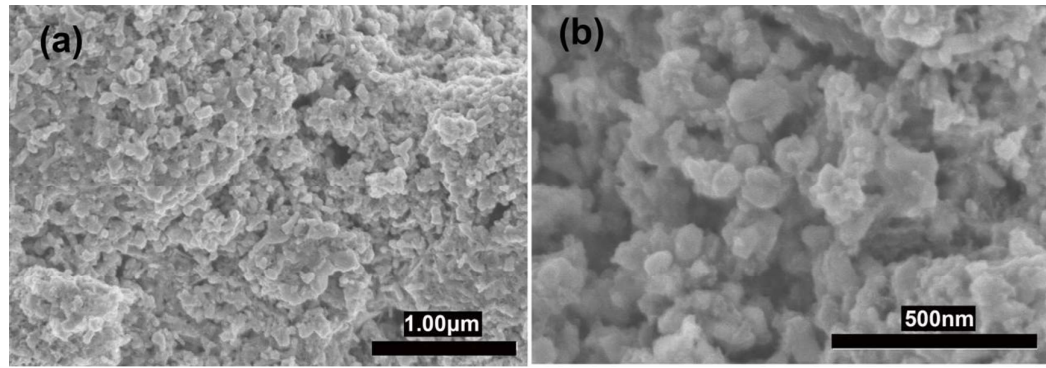
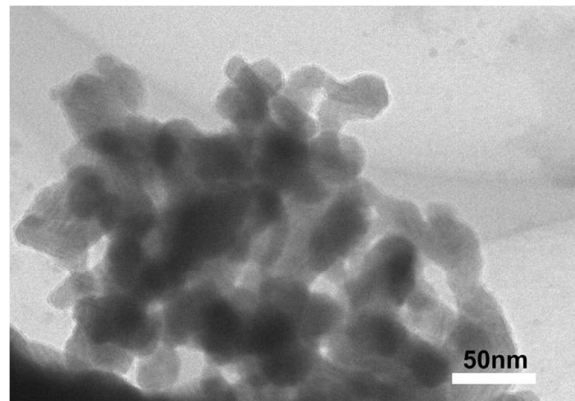


Figure S2. (a) and (b) SEM images of MoP/Mo₂C@C annealed at 800 °C for 6 hour under N_2 atmosphere. The images showed that as-synthesized superstructure was assembled from MoP/Mo₂C@C nanoparticles.



FigureS3. TEM image of P_4Mo_6 annealed without DCA (MoP/MoC_x), confirming that the nanoparticles without graphitic carbon shells aggregate with each other.

Table S1. The P, Mo, C, N, and O components of $MoP/Mo_2C@C$ recorded from the EDX quantitative analyses (three parallel measurements).

	1		2		3		Average	
	Weight %	Atoms %						
P	19.17	20.66	16.56	16.01	17.02	15.02	17.58	17.23
Mo	58.42	20.33	54.34	16.96	49.33	14.06	54.03	17.12
C	17.45	48.51	19.97	49.8	23.29	52.99	20.23	50.43
N	0.49	1.17	0.45	0.96	0.96	1.86	0.63	1.33
O	4.47	9.33	8.69	16.26	9.41	16.07	7.52	13.88

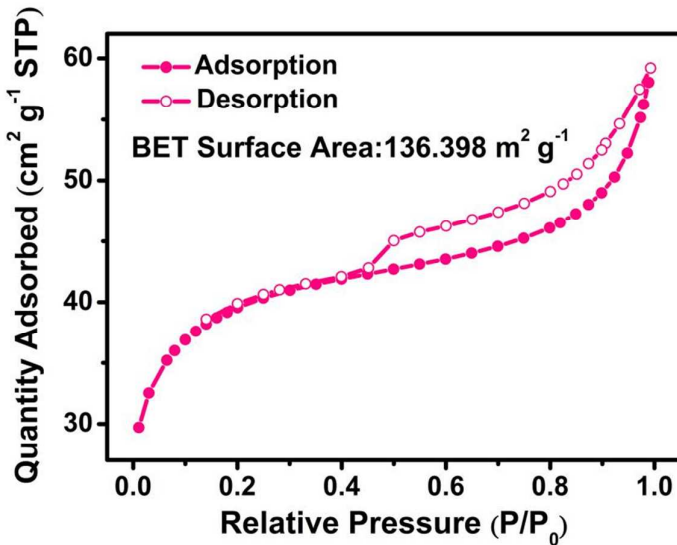


Figure S4. N₂ sorption isotherm of MoP/Mo₂C@C. The results suggest that the electrocatalyst possesses a mesoporous structure.

Table S2. Comparison of HER performance in acidic media for MoP/Mo₂C@C with other HER electrocatalysts.

Catalyst	Current density (mA cm ⁻²)	Overpotential (mV)	Tafel			Ref.
			slo pe (mV dec ⁻¹)	J _o (mA cm ⁻²))	
MoP/Mo₂C@C	10	89	45	0.215	This work	
(MoS ₂) _{0.6} (SnO ₂) _{0.4} /rGO	10	263	50.8	N.A.	[S1]	
MoP-CA2	10	125	54	0.086	[S2]	
MoP	10	150	50	0.01	[S3]	
MoP/CF	10	200	56.4	N.A.	[S4]	

3D MoP	10	105	126	3.052	[S5]
Mo-W-P/CC	100	138	52	0.288	[S6]
MoS ₂	10	203	60	N.A.	[S7]
Mo ₂ C@NC	10	124	60	0.096	[S8]
Mo ₂ C/CC	10	140	124	N.A.	[S9]
MoCx	10	142	53	0.023	[S10]
Mo ₂ C-RGO	10	130	57.3	N.A.	[S11]
np-Mo ₂ C NWS	60	200	53	N.A.	[S12]
Mo ₂ C-NCNT	10	147	71	0.114	[S13]
MoB	17	250	55	0.0014	[S14]
MoCN	10	140	46	N.A.	[S15]
MoS ₂	10	103	49	0.00962	[S16]
MoN	38.5	300	90	0.0837	[S17]
MoP NPs	10	90	45	0.12	[S18]

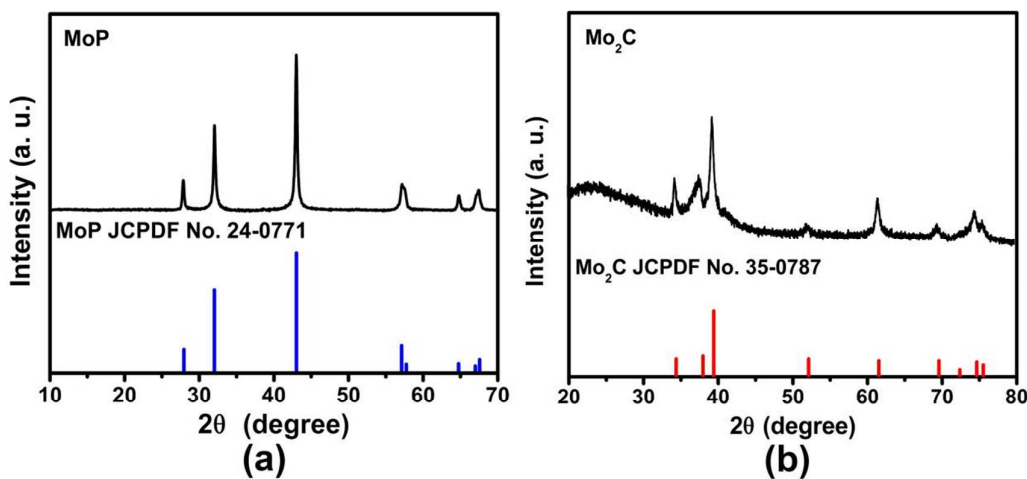


Figure S5. Powder XRD patterns of (a) MoP and (b) Mo₂C.

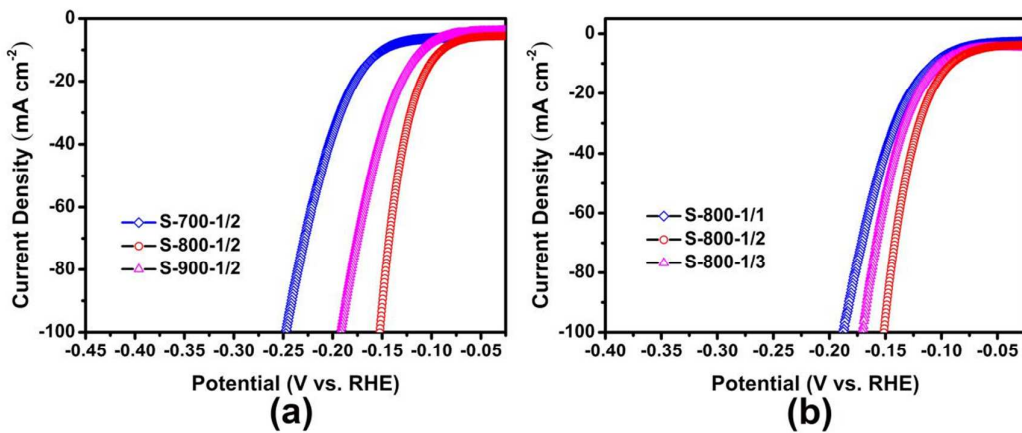


Figure S6. (a) Polarization curves of samples with same mass ratio 1/2 annealed at different temperature of 700, 800 and 900 °C in 0.5 M H₂SO₄. The results indicated that different pyrolysis temperature have a great effect on the electrocatalytic performance of catalysts and the most optimal pyrolysis temperature is 800 °C; (b) Polarization curves of samples annealed at 800 °C with different mass ratio of starting materials (P₄Mo₆/DCA) of 1/1, 1/2 and 1/3 in 0.5 M H₂SO₄; The results showed that the mass ratio of POM precursor and DCA have an influence on the electrocatalytic performance of catalysts and the most optimal weight ratio is found to be 1:2.

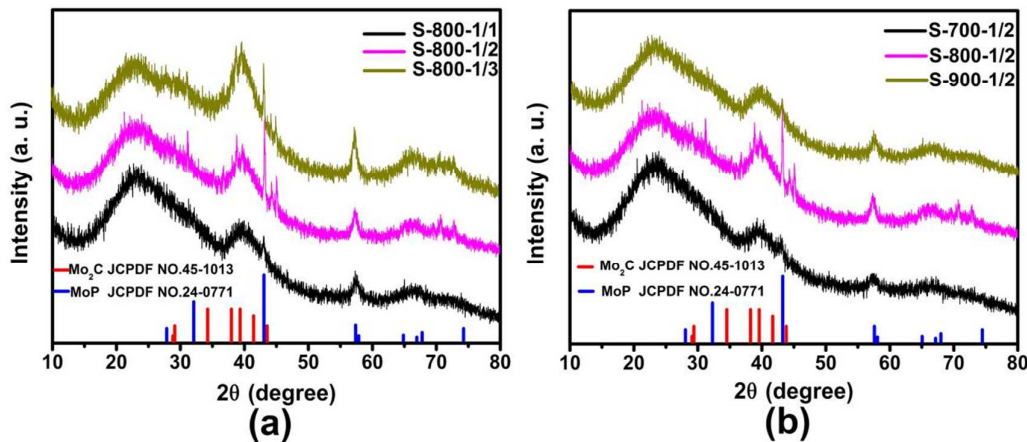


Figure S7. (a) Powder XRD patterns of samples annealed at 800 °C with different mass ratio of starting materials (P₄Mo₆/DCA) of 1/1, 1/2 and 1/3; (b) Powder XRD patterns of samples with same mass ratio 1/2 annealed at different temperature of 700, 800 and 900 °C.

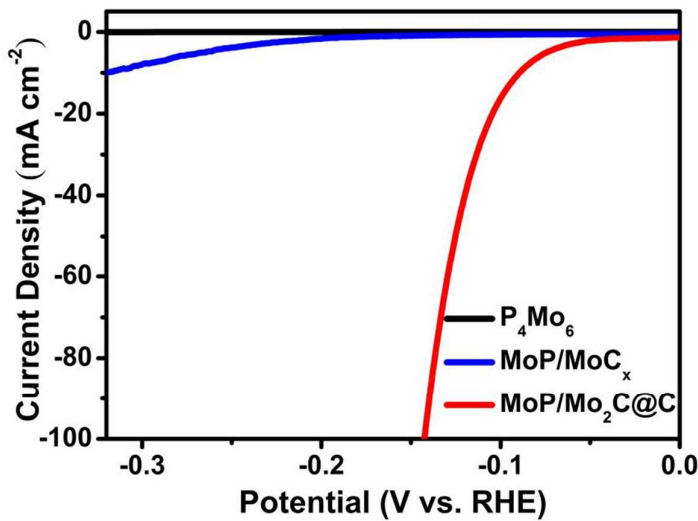


Figure S8. Polarization curves of $\text{MoP}/\text{Mo}_2\text{C}@\text{C}$, P_4Mo_6 precursor, and P_4Mo_6 annealed without DCA in 0.5 M H_2SO_4 (MoP/MoC_x), the results suggest the function of few-layer graphitic carbon shells.

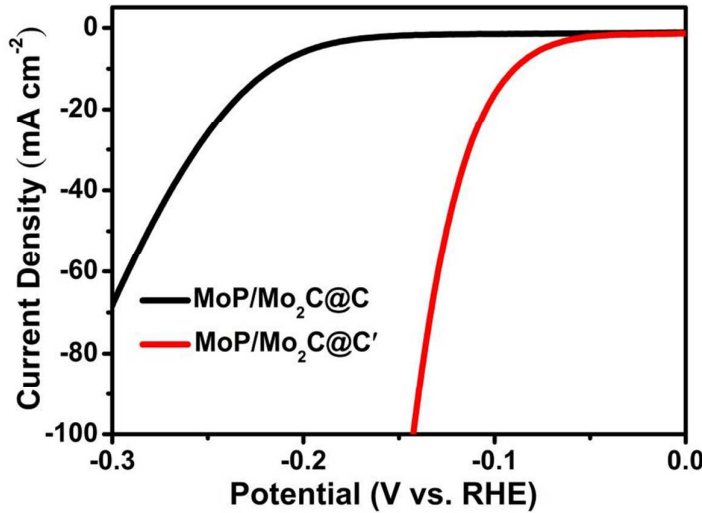


Figure S9. Polarization curves of $\text{MoP}/\text{Mo}_2\text{C}@\text{C}$, $\text{MoP}/\text{Mo}_2\text{C}@\text{C}'$ (without N-doped in graphitic carbon shells) in 0.5 M H_2SO_4 , the results suggest the function of N dopant for HER performance.

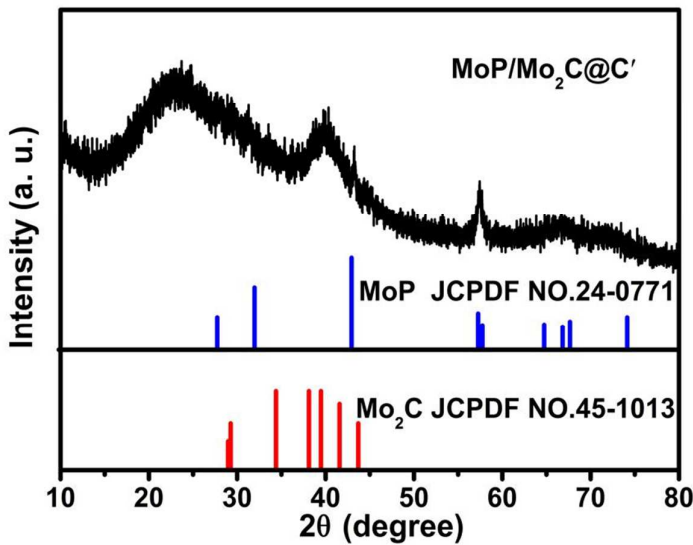


Figure S10. Powder XRD patterns of $\text{MoP}/\text{Mo}_2\text{C}@\text{C}'$ (without N-doped in graphitic carbon shells).

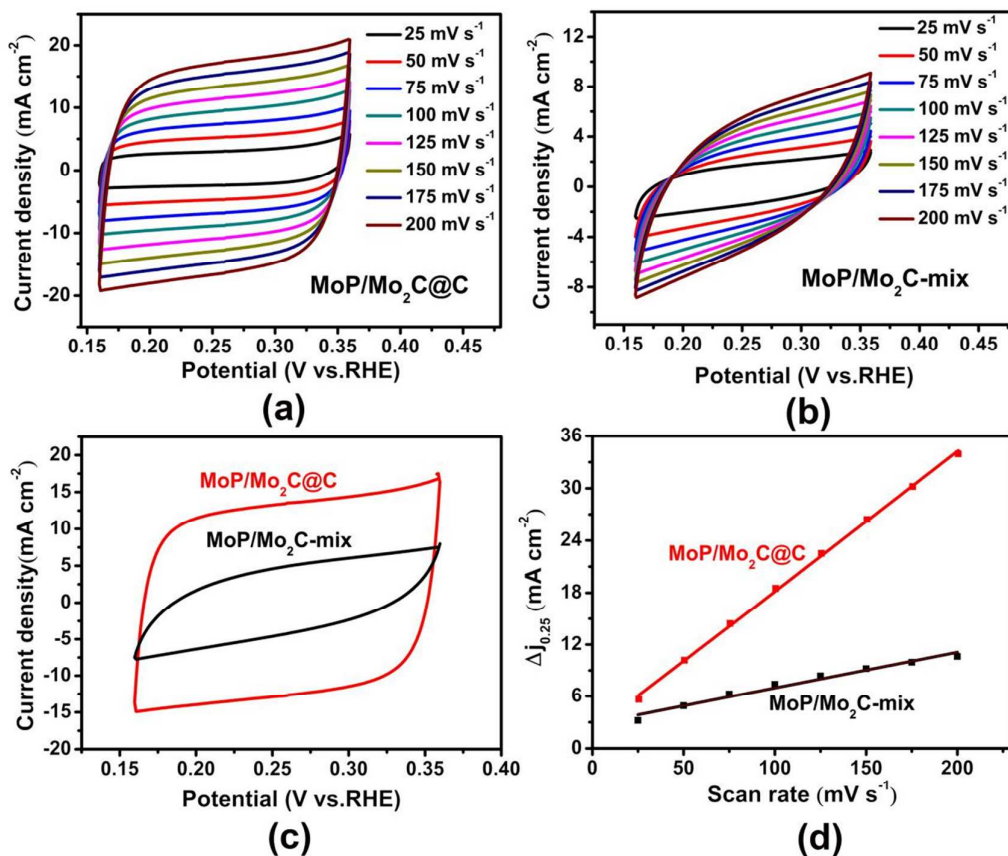


Figure S11. Cyclic voltammograms (CVs) of (a) $\text{MoP}/\text{Mo}_2\text{C}@\text{C}$ and (b) $\text{MoP}/\text{Mo}_2\text{C}$ -mix in the potential range from 0.16 to 0.36 V without redox current

peaks in 0.5M H₂SO₄; (c) comparison of the CV curves of MoP/Mo₂C@C and MoP/Mo₂C-mix at 150 mV s⁻¹ within the same potential region; (d) Linear fitting of Δj of both samples ($\Delta j = j_a - j_c$) vs. scan rates at a given potential of +0.25 V vs. RHE. j_a is the anodic current density and j_c is the cathodic current density, respectively.

Table S3. The values of charge transfer resistance (Rct) and a series resistance (Rs) for MoP/Mo₂C@C with overpotential from 50 to 250 mV in 0.5 M H₂SO₄.

Potential (mV vs. RHE)	MoP/Mo ₂ C@C	
	Rct (Ω)	Rs (Ω)
50	1732	8.175
100	483.9	8.058
150	87.02	7.484
200	16.59	7.846
250	7.08	8.23

Table S4. Comparison of HER performance in alkaline media for MoP/Mo₂C@C with other HER elecrocatalysts.

Catalyst	Current density (mA cm ⁻²)	Overpotential (mV)	Tafel slope (mV dec ⁻¹)	J_o (mA cm ⁻²)	Ref.
MoP/Mo₂C@C	10	75	58	0.53	This work
MoCx	10	151	59	0.029	[S10]
Mo ₂ C-NCNT	10	257	N.A.	N.A.	[S13]
MoB	5	250	59	0.002	[S14]
MoS ₂ NiS MoO ₃	10	91	70	N.A.	[S19]

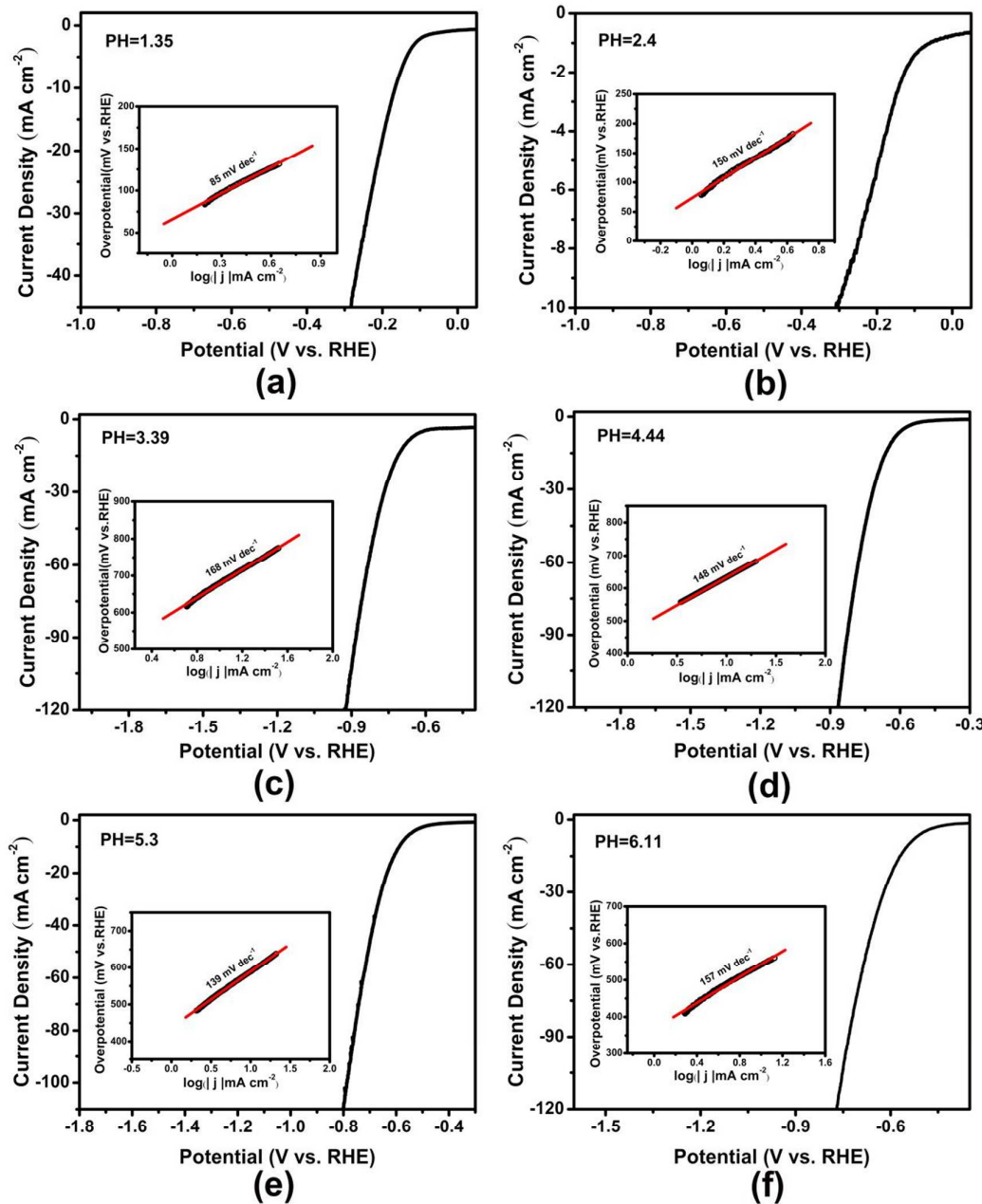


Figure S12. The HER polarization plots of MoP/Mo₂C@C in pH 1.35 (a), 2.4 (b), 3.39 (c), 4.44 (d), 5.3 (e) and 6.11 (f) electrolytes at scan rate of 5 mV s⁻¹. Insert: The corresponding Tafel plots of MoP/Mo₂C@C.

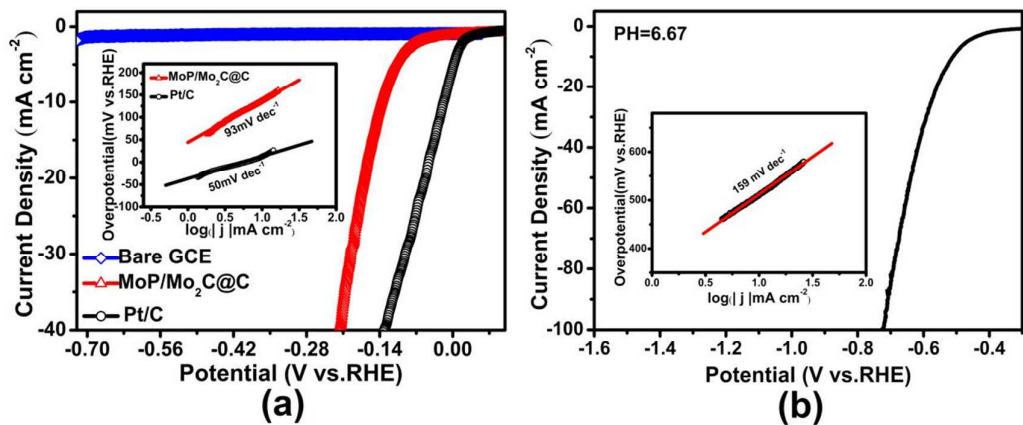


Figure S13. The HER polarization plots of MoP/Mo₂C@C in 1 M PBS(pH=7)(a), pH=6.67(Na₂SO₄) (b) electrolytes at scan rate of 5 mV s⁻¹. Insert: The corresponding Tafel plots of MoP/Mo₂C@C.

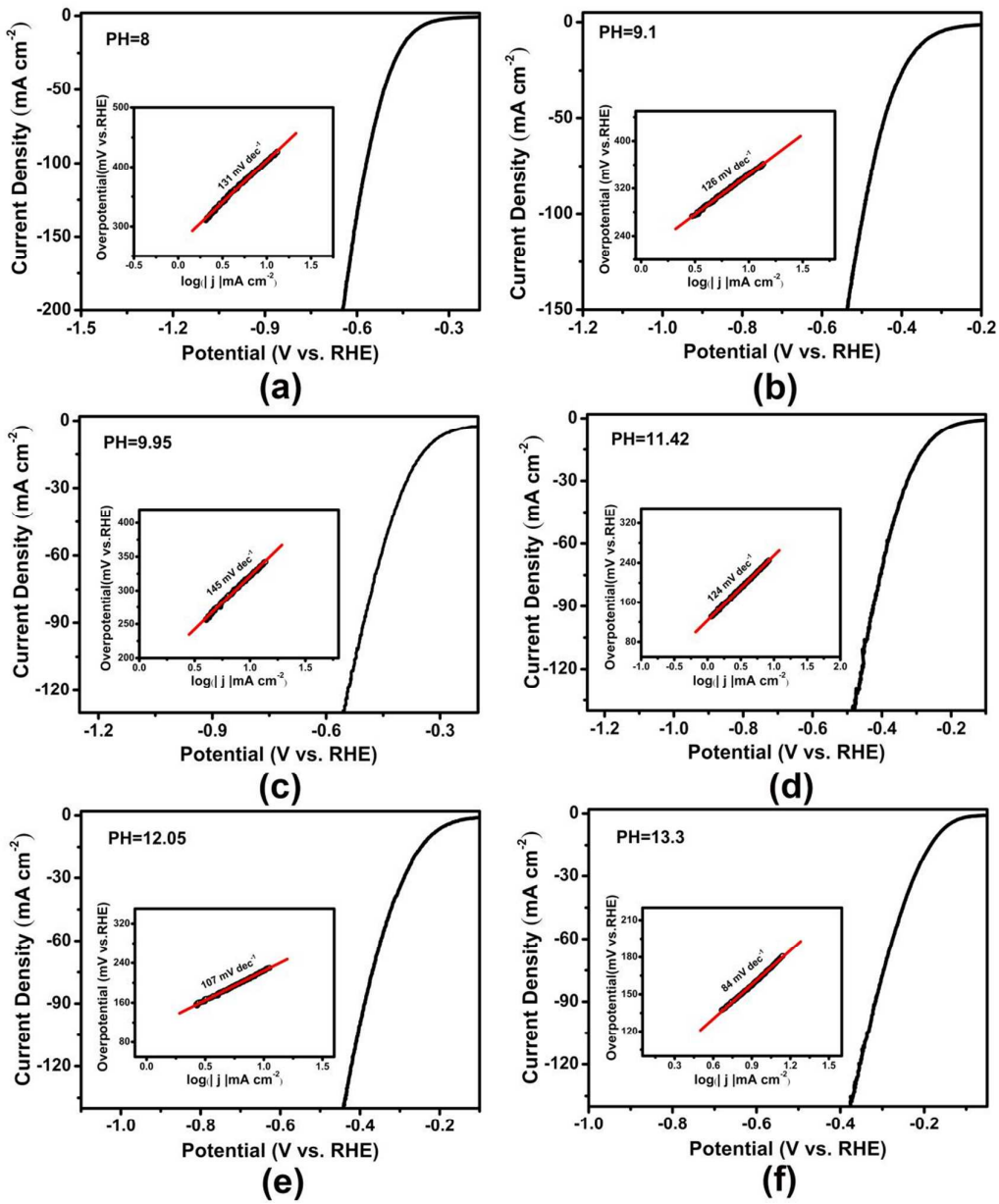


Figure S14. The HER polarization plots of MoP/Mo₂C@C in pH 8 (a), 9.1 (b), 9.95 (c), 11.42 (d), 12.05 (e) and 13.3 (f) electrolytes at scan rate of 5 mV s⁻¹. Insert: The corresponding Tafel plots of MoP/Mo₂C@C.

Table S5. Comparison of catalytic parameters of MoP/Mo₂C@C in different electrolytes.

pH value	Overpotential at 10 mA cm ⁻² (mV vs RHE)	Tafel slope (mV dec ⁻¹)
0.3	89	45
1.3	155	85
2.4	293	150
3.3	670	168
4.4	624	148
5.3	578	139
6.1	530	157
7.0(1 M PBS)	136	93
6.67(Na ₂ SO ₄)	510	159
8.0	401	131
9.1	334	126
9.9	310	145
11.4	245	124
12.1	213	107
13.3	156	84
14.0	75	58

Additional experimental data:

The nanocomposites synthesized with a P₄Mo₆/DCA ratio of 1:2 at 800 °C also show the best HER performance in pH =14 (1 M KOH) and PH=7 (1 M PBS), as shown in Figure S15, S16.

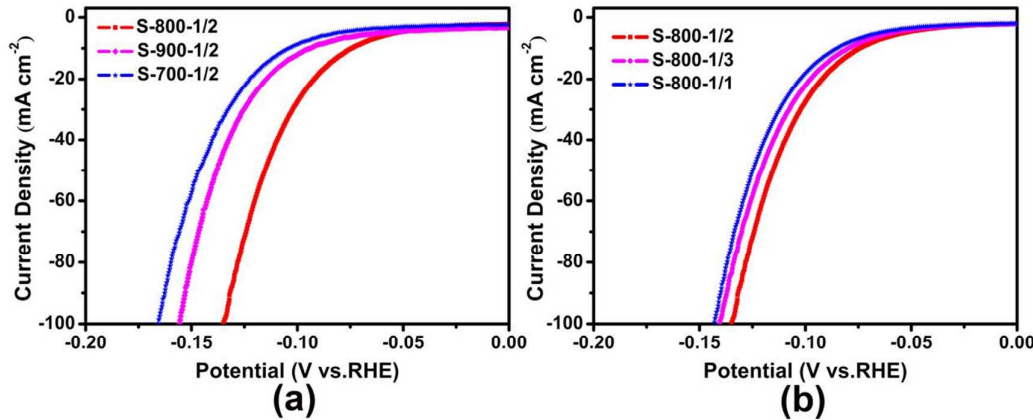


Figure S15. (a) Polarization curves of samples with same mass ratio 1/2 annealed at different temperature of 700, 800 and 900 °C in 1 M KOH; (b) Polarization curves of samples annealed at 800 °C with different mass ratio of starting materials (P₄Mo₆/DCA) of 1/1, 1/2 and 1/3 in 1 M KOH. These results showed that the nanocomposites synthesized with a P₄Mo₆/DCA ratio of 1:2 at 800 °C showed the best HER performance in 1 M KOH.

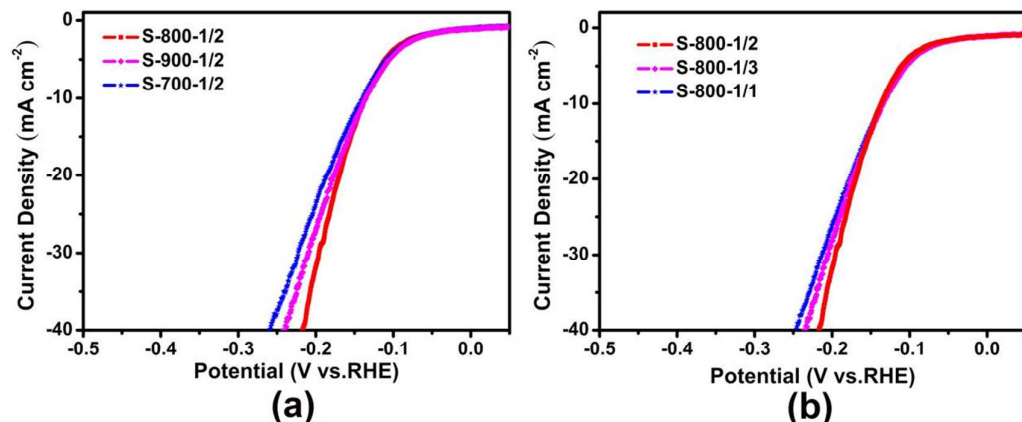


Figure S16. (a) Polarization curves of samples with same mass ratio 1/2 annealed at different temperature of 700, 800 and 900 °C in 1 M PBS (PH=7); (b) Polarization curves of samples annealed at 800 °C with different mass ratio of starting materials (P₄Mo₆/DCA) of 1/1, 1/2 and 1/3 in 1 M PBS (PH=7). These results showed that the

nanocomposites synthesized with a P₄Mo₆/DCA ratio of 1:2 at 800 °C showed the best HER performance in 1 M PBS (PH=7).

To further explore the durability of the nanocomposites, the powder XRD and TEM characterizations of MoP/Mo₂C@C after 1000 cycles of stability tests have been performed. These results reveal that the structure and phase of MoP/Mo₂C@C can be remained after stability tests.

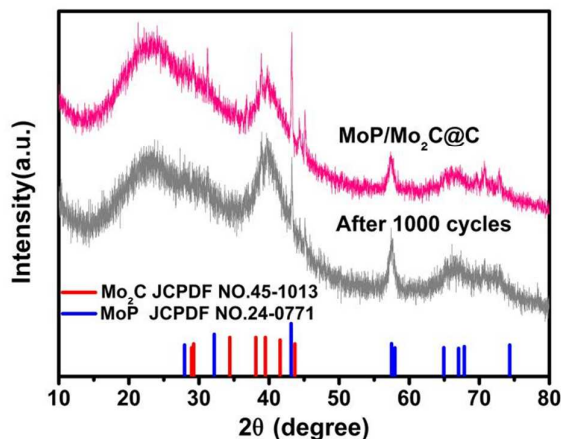


Figure S17. The PXRD patterns of MoP/Mo₂C@C (pink line) and after 1000 cycles (gray line). These results reveal that the structure of MoP/Mo₂C@C can be remained after 1000 cycles HER test.

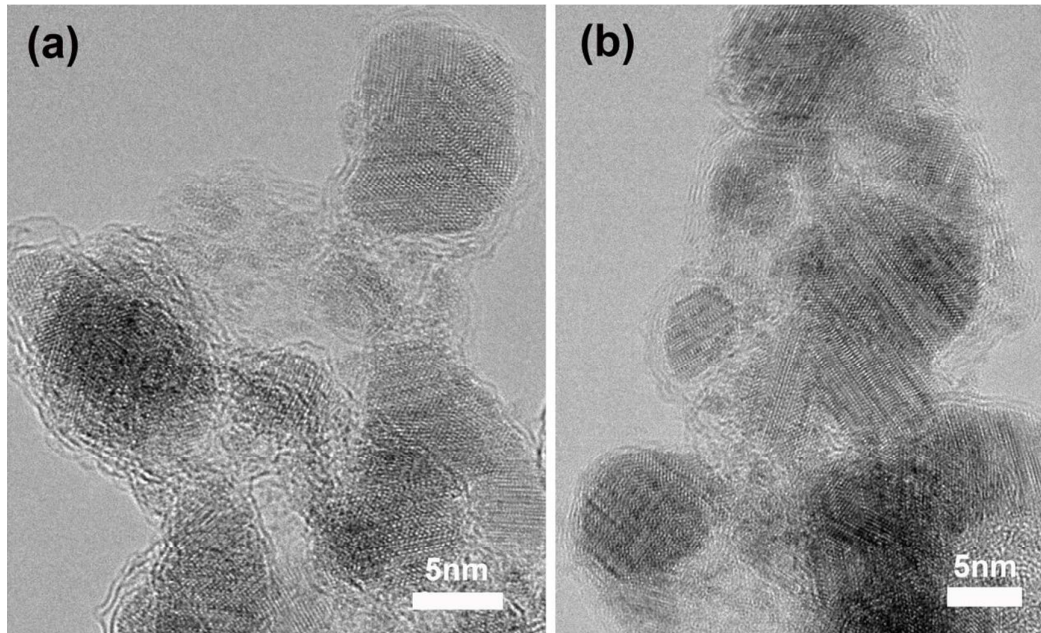


Figure S18. (a) and (b) TEM images of MoP/Mo₂C@C after 1000 cycles test. The images show that the morphology of MoP/Mo₂C@C catalyst shows negligible changes.

In order to illustrate the composition of the electrocatalyst, the SEM element distribution mapping of P, Mo, C, and N are shown in the figure below.

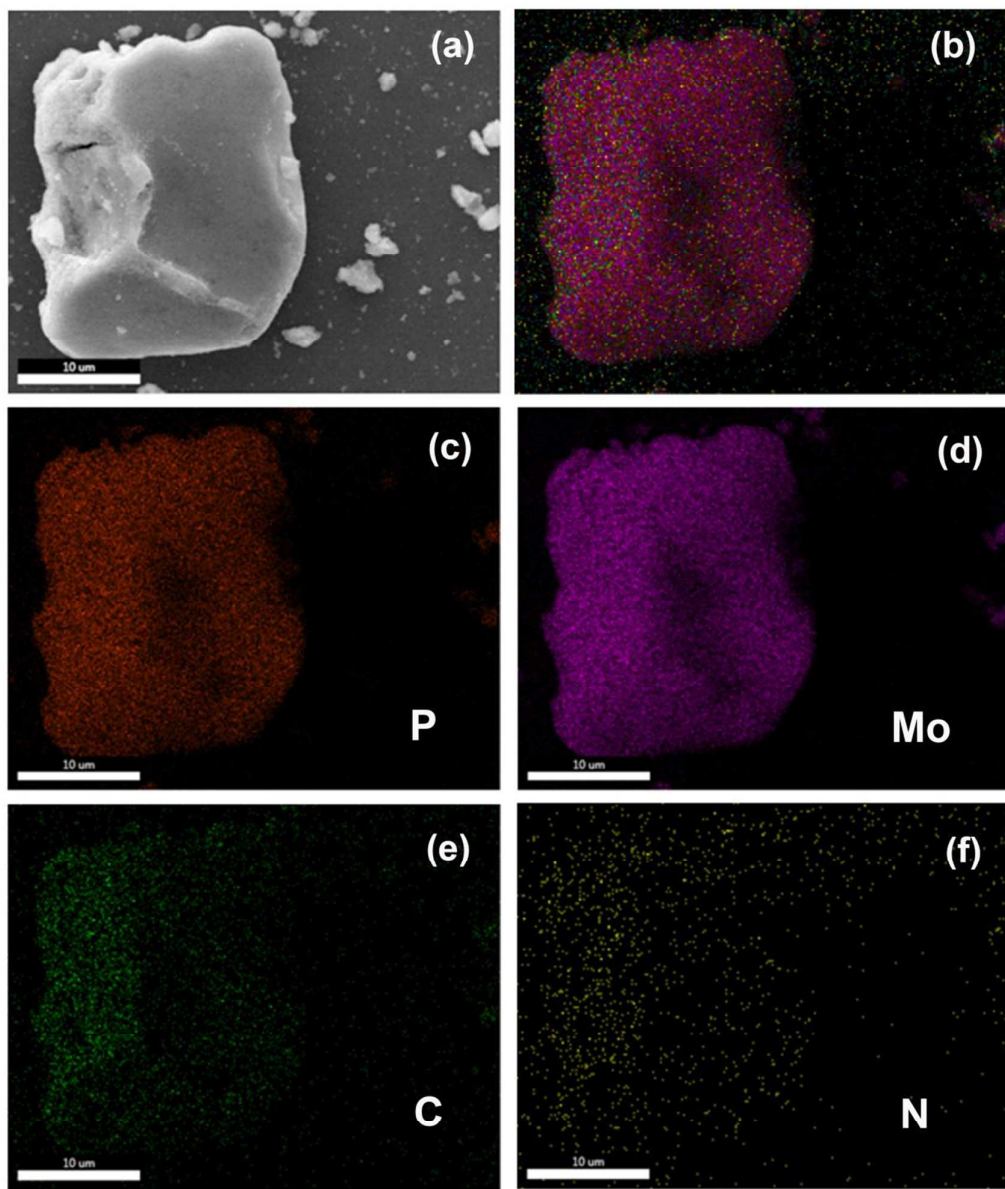


Figure S19. (a)-(f) corresponding EDX elemental mapping of P, Mo, C and N in MoP/Mo₂C@C.

Supplementary References

- [S1] Ravula, S.; Zhang, C.; Essner, J. B.; Robertson, J. D.; Lin, J.; Baker, G. A. Ionic Liquid-Assisted Synthesis of Nanoscale $(\text{MoS}_2)_x(\text{SnO}_2)_{1-x}$ on Reduced Graphene Oxide for the Electrocatalytic Hydrogen Evolution Reaction. *ACS Appl. Mater. Interfaces.* **2017**, *9*, 8065-8074.
- [S2] Xing, Z. C.; Liu, Q.; Asiri, A. M.; Sun, X. P. Closely Interconnected Network of Molybdenum Phosphide Nanoparticles: A Highly Efficient Electrocatalyst for Generating Hydrogen from Water. *Adv. Mater.* **2014**, *26*, 5702-5707.
- [S3] Wang, T. Y.; Du, K. Z.; Liu, W. L.; Zhu, Z. W.; Shao, Y. H.; Li, M. X. Enhanced Electrocatalytic Activity of MoP Microparticles for Hydrogen Evolution by Grinding and Electrochemical Activation. *J. Mater. Chem. A.* **2015**, *3*, 4368-4373.
- [S4] Cui, W.; Liu, Q.; Xing, Z. C.; Asiri, A. M.; Alamry, K. A.; Sun, X. P. MoP Nanosheets Supported on Biomass-Derived Carbon Flake: One-Step Facile Preparation and Application as a Novel High-Active Electrocatalyst toward Hydrogen Evolution Reaction. *Appl. Catal. B-Environ.* **2015**, *164*, 144-150.
- [S5] Deng, C.; Ding, F.; Li, X. Y.; Guo, Y. F.; Ni, W.; Yan, H.; Sun, K. N.; Yan, Y. M. Templated-Preparation of a Three-Dimensional Molybdenum Phosphide Sponge as a High Performance Electrode for Hydrogen Evolution. *J. Mater. Chem. A.* **2016**, *4*, 59-66.
- [S6] Wang, X. D.; Xu, Y. F.; Rao, H. S.; Xu, W. J.; Chen, H. Y.; Zhang, W. X.; Kuang, D. B.; Su, C. Y. Novel Porous Molybdenum Tungsten Phosphide Hybrid Nanosheets on Carbon Cloth for Efficient Hydrogen Evolution. *Energy Environ. Sci.* **2016**, *9*, 1468-1475.
- [S7] Ma, R. G.; Zhou, Y.; Chen, Y. F.; Li, P. X.; Liu, Q.; Wang, J. C. Ultrafine Molybdenum Carbide Nanoparticles Composited with Carbon as a Highly Active Hydrogen-Evolution Electrocatalyst. *Angew. Chem. Int. Ed.* **2015**, *54*, 14723-14727.
- [S8] Liu, Y. P.; Yu, G. T.; Li, G. D.; Sun, Y. H.; Asefa, T.; Chen, W. Zou, X. X. Coupling Mo₂C with Nitrogen-Rich Nanocarbon Leads to Efficient Hydrogen-Evolution Electrocatalytic Sites. *Angew. Chem. Int. Ed.* **2015**, *54*, 10752-10757.
- [S9] Fan, M. H.; Chen, H.; Wu, Y. Y.; Feng, L. L.; Liu, Y. P.; Li, G. D.; Zou, X. X. Growth of Molybdenum Carbide Micro-Islands on Carbon Cloth toward Binder-Free Cathodes for Efficient Hydrogen Evolution Reaction. *J. Mater. Chem. A.* **2015**, *3*, 16320-16326.
- [S10] Wu, H. B.; Xia, B. Y.; Yu, L.; Yu, X. Y.; Lou, X. W. Porous Molybdenum Carbide

Nano-Octahedrons Synthesized via Confined Carburization in Metal-Organic Frameworks for Efficient Hydrogen Production *Nat. Commun.*, **2015**, *6*, 6512-6519.

[S11] Pan, L. F.; Li, Y. H.; Yang, S.; liu, P. F.; Yu, M. Q.; Yang, H. G. Molybdenum Carbide Stabilized on Graphene with High Electrocatalytic Activity for Hydrogen Evolution Reaction. *Chem. Commun.* **2014**, *50*, 13135-13137.

[S12] Liao, L.; Wang, S. N.; Xiao J. J.; Bian, X. J.; Zhang, Y. H.; Scanlon, M. D.; Hu, X. L.; Tang, Y.; Liu, B. H.; Girault, H. H. A Nanoporous Molybdenum Carbide Nanowire as an Electrocatalyst for Hydrogen Evolution Reaction. *Energy Environ. Sci.* **2014**, *7*, 387-392.

[S13] Zhang, K.; Zhao, Y.; Fu, D. Y.; Chen, Y. J. Molybdenum Carbide Nanocrystal Embedded N-Doped Carbon Nanotubes as Electrocatalysts for Hydrogen Generation. *J. Mater. Chem. A.* **2015**, *3*, 5783-5788.

[S14] Vrubel, H.; Hu, X. L. Molybdenum Boride and Carbide Catalyze Hydrogen Evolution in both Acidic and Basic Solutions. *Angew. Chem. Int. Ed.* **2012**, *51*, 12703-12706.

[S15] Zhao, Y.; Kamiya, K.; Hashimoto, K.; Nakanishi, S. In Situ CO₂-Emission Assisted Synthesis of Molybdenum Carbonitride Nanomaterial as Hydrogen Evolution Electrocatalyst. *J. Am. Chem. Soc.* **2015**, *137*, 110-113.

[S16] Gao, M. R.; Chan, M. K. Y.; Sun, Y. G. Edge-Terminated Molybdenum Disulfide with a 9.4-Å Interlayer Spacing for Electrochemical Hydrogen Production. *Nat. Commun.* **2015**, *6*, 7493-7500.

[S17] Xie, J. F.; Li, S.; Zhang, X. D.; Zhang, J. J.; Wang, R. X.; Zhang, H.; Pan B. C.; Xie, Y. Atomically-Thin Molybdenum Nitride Nanosheets with Exposed Active Surface Sites for Efficient Hydrogen Evolution. *Chem. Sci.* **2014**, *5*, 4615-4620.

[S18] McEnaney, J. M.; Crompton, J. C.; Callejas, J. F.; Popczun, E. J.; Biacchi, A. J.; Lewis, N. S.; Schaak, R. E. Amorphous Molybdenum Phosphide Nanoparticles for Electrocatalytic Hydrogen Evolution. *Chem. Mater.* **2014**, *26*, 4826-4831.

[S19] Wang, C. Q.; Tian, B.; Wu, M.; Wang, J. H. Revelation of the Excellent Intrinsic Activity of MoS₂|NiS|MoO₃ Nanowires for Hydrogen Evolution Reaction in Alkaline Medium. *ACS Appl. Mater. Interfaces.* **2017**, *9*, 7084-7090.